SUPPLEMENTARY INFORMATION

First Achieving Highly Selective Oxidation of Aliphatic Alcohols to Aldehydes over Photocatalysts

Feng Xie[†, ‡], Yin Zhang[‡], Xiao He[‡], Hongdong Li[‡], Xueying Qiu[‡], Wencai Zhou[‡], Shutong Huo[§], Zhiyong Tang[‡ *]

[†] Advanced Membranes and Porous Materials Center, Physical Sciences and Engineering Division, King Abdullah University of Science and Technology, Thuwal 23955-6900, Saudi Arabia

[‡] Chinese Academy of Sciences Key Laboratory of Nanosystem and Hierarchical Fabrication, National Center for Nanoscience and Technology, Chinese Academy of Sciences, Beijing 100190, P. R. China

[§] Department of Health Policy and Management, Yale School of Public Health, Yale University, New Haven, CT, 06520-8018, USA

[*] Corresponding author. Email: zytang@nanoctr.cn

The PDF file includes:

Figure S1. SEM image of single BiOBr microsphere and the corresponding EDX elemental mapping of Bi (green), O (blue), and Br (red). The scale bars on the Bi, O, and Br images are the same as that on the SEM image.

Figure S2. SEM image of single BiOI microsphere and the corresponding EDX elemental mapping of Bi (red), O (blue), and I (green). The scale bars on the Bi, O, and I images are the same as that on the SEM image.

Figure S3. (a) N_2 adsorption-desorption isotherms of BiOBr samples. (b) N_2 adsorption-desorption isotherms of BiOI samples.

Figure S4. (a) XPS survey spectrum of BiOCl, BiOBr, and BiOI. (b) Mott-Schottky plots of BiOCl samples. (c) Mott-Schottky plots of BiOBr samples. (d) Mott-Schottky plots of BiOI samples. **C** represents the capacitance, and **E** is the applied potential.

Figure S5. The cyclic voltammogram of alcohols (left) and aldehydes (right) with different concentrations (0.1, 0.2, and 0.5 mM).

Figure S6. GC result for 1-Hexanol selectively oxidation to Caproaldehyde over BiOCl under light irradiation at 25 °C.

Figure S7. GC result for 1-Hexanol selectively oxidation to Caproaldehyde over BiOCl without oxygen (N_2 atmosphere) under light irradiation at 25 °C.

Figure S8. MS spectrum of Valeraldehyde.

Figure S9. MS spectrum of Caproaldehyde.

Figure S10. MS spectrum of Heptaldehyde.

Figure S11. Photoreaction equipment of photocatalytic experiment process.

Figure S12. Fluorescence detection of the generated H_2O_2 after oxidation reaction over BiOCl, BiOBr, and BiOI.

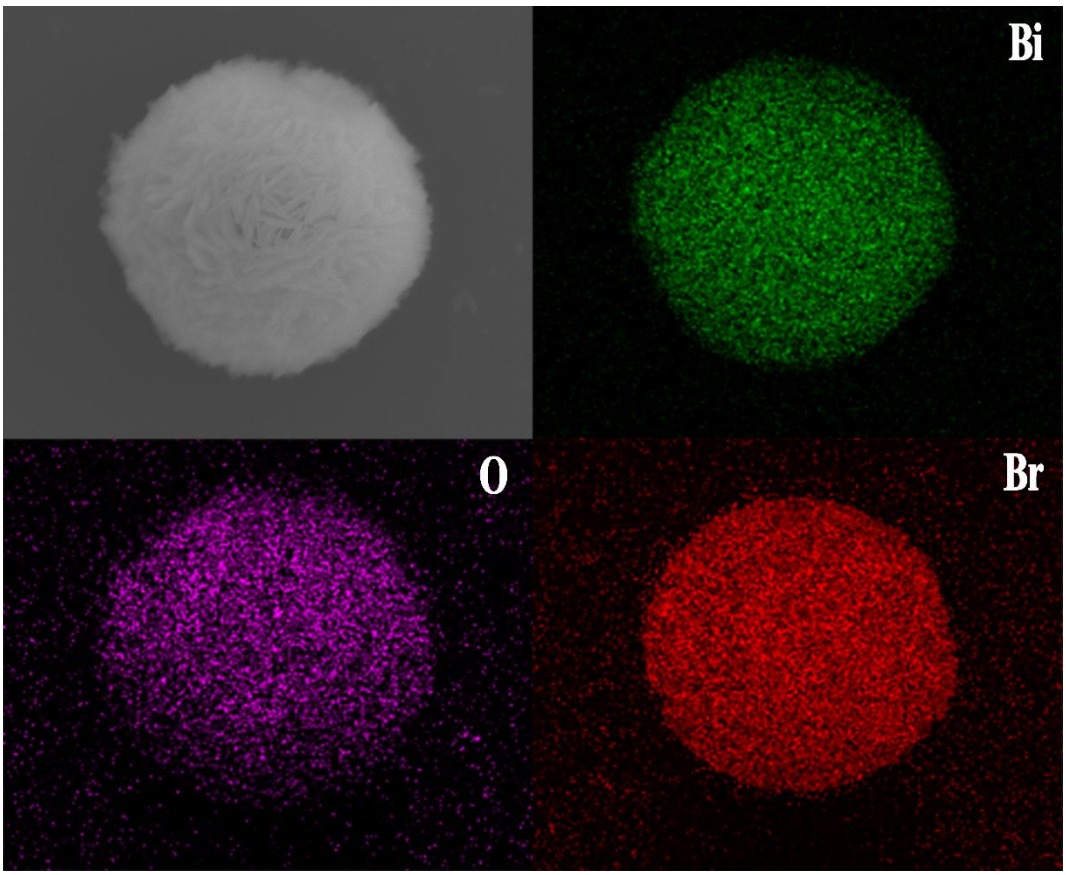

Figure S1. SEM image of a single BiOBr microsphere and the corresponding EDX elemental mapping of Bi (green), O (blue), and Br (red). The scale bars on the Bi, O, and Br images are the same as that on the SEM image.

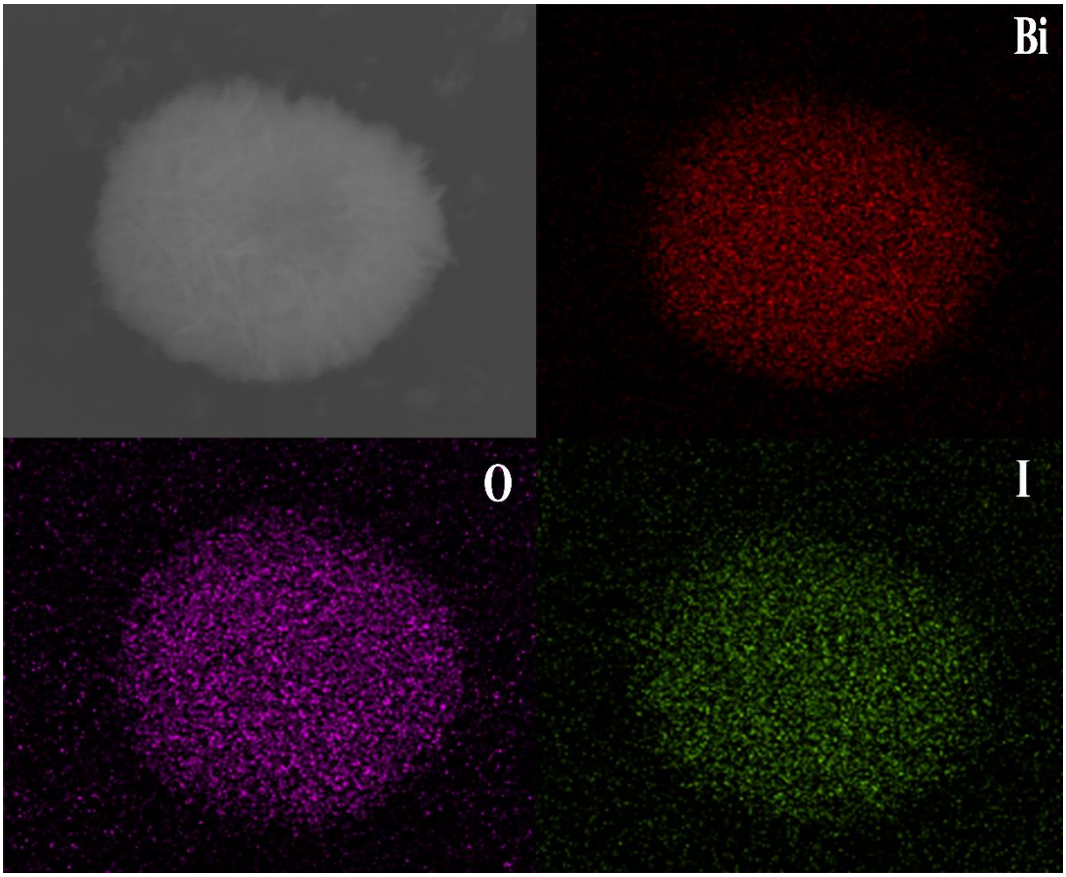

Figure S2. SEM image of a single BiOI microsphere and the corresponding EDX elemental mapping of Bi (red), O (blue), and I (green). The scale bars on the Bi, O, and I images are the same as that on the SEM image.

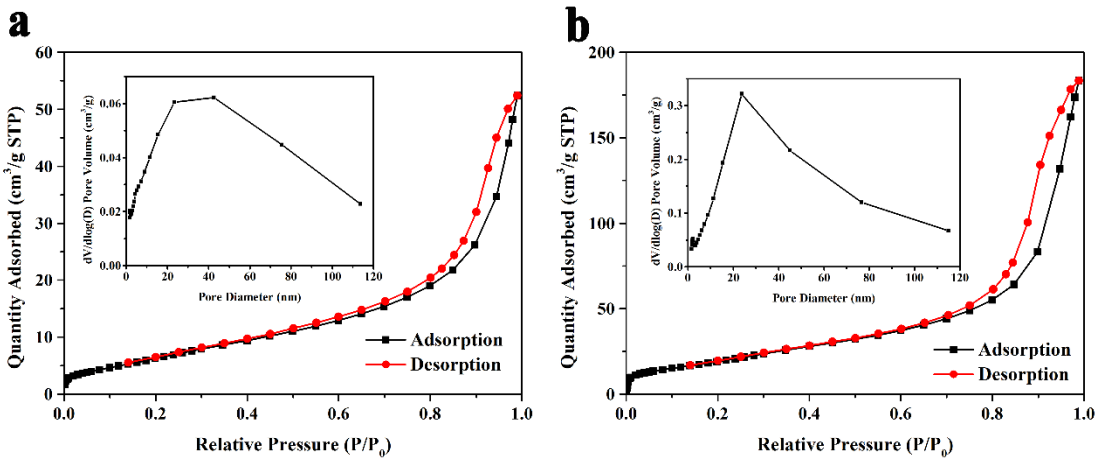

Figure S3. (a) N_2 adsorption-desorption isotherms of BiOBr samples. (b) N_2 adsorption-desorption isotherms of BiOI samples.

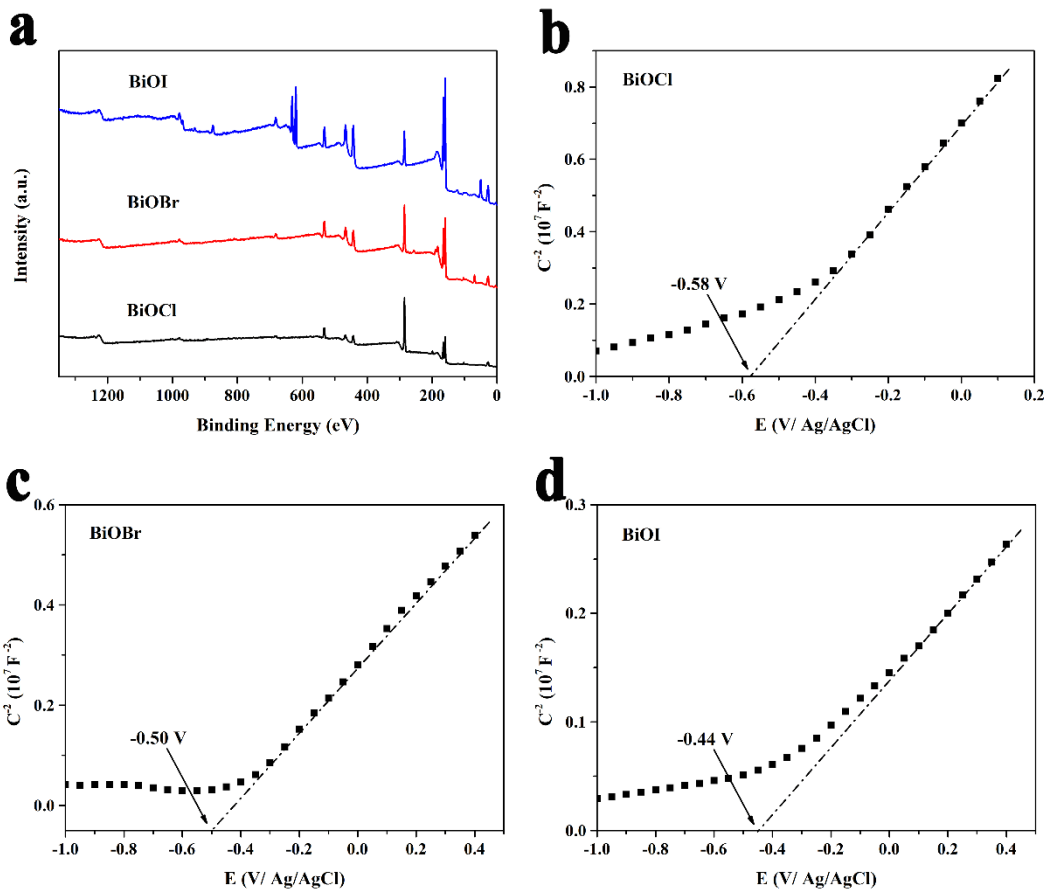

Figure S4. (a) XPS survey spectrum of BiOCl, BiOBr, and BiOI. (b) Mott-Schottky plots of BiOCl samples. (c) Mott-Schottky plots of BiOBr samples. (d) Mott-Schottky plots of BiOI samples. **C** represents the capacitance, and **E** is the applied potential.

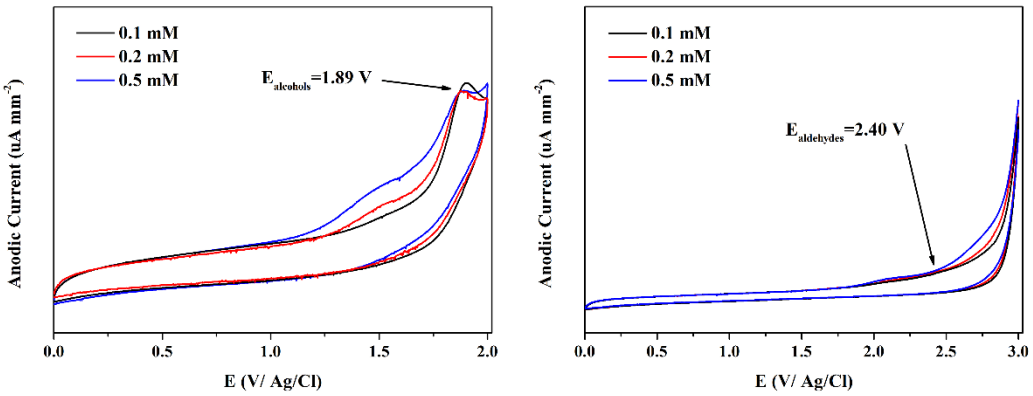

Figure S5. The cyclic voltammogram of alcohols (left) and aldehydes (right) with different concentrations (0.1, 0.2, and 0.5 mM).

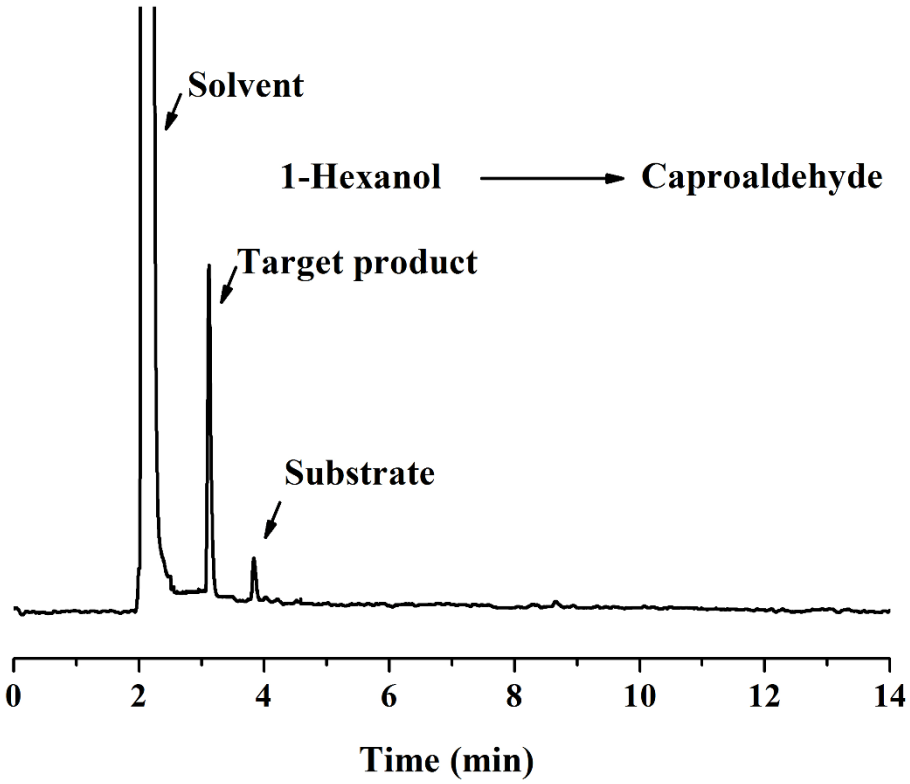

Figure S6. GC result for 1-Hexanol selectively oxidation to Caproaldehyde over BiOCl under light irradiation at 25 °C.

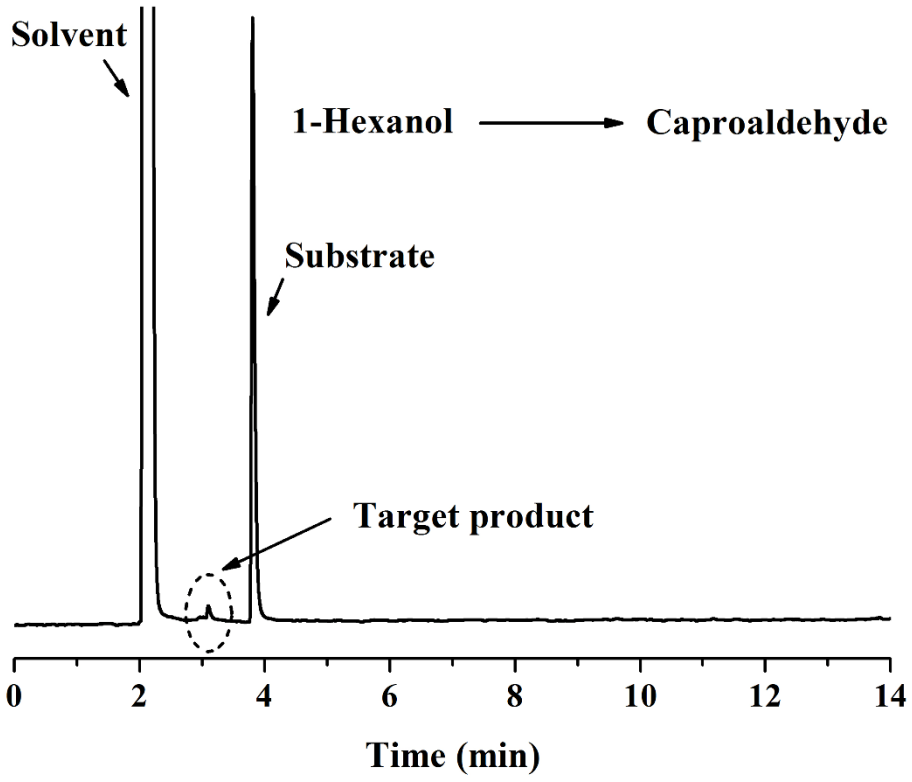

Figure S7. GC result for 1-Hexanol selectively oxidation to Caproaldehyde over BiOCl without molecular oxygen (N_2 atmosphere) under light irradiation at 25 °C.

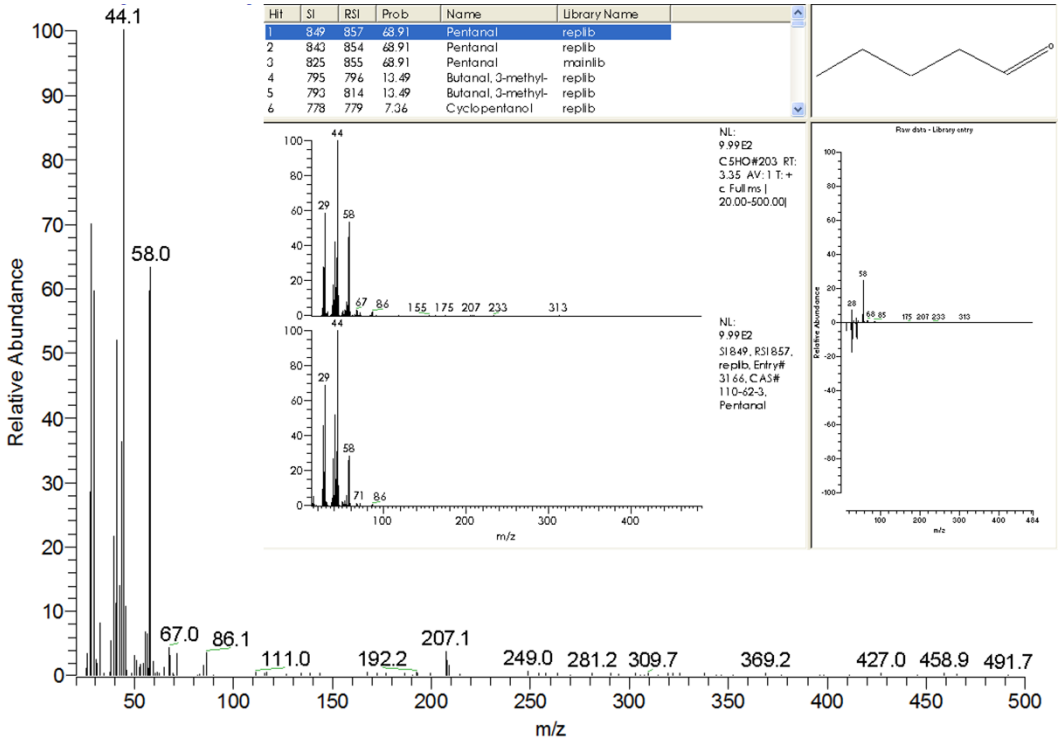

Figure S8. MS spectrum of Valeraldehyde.

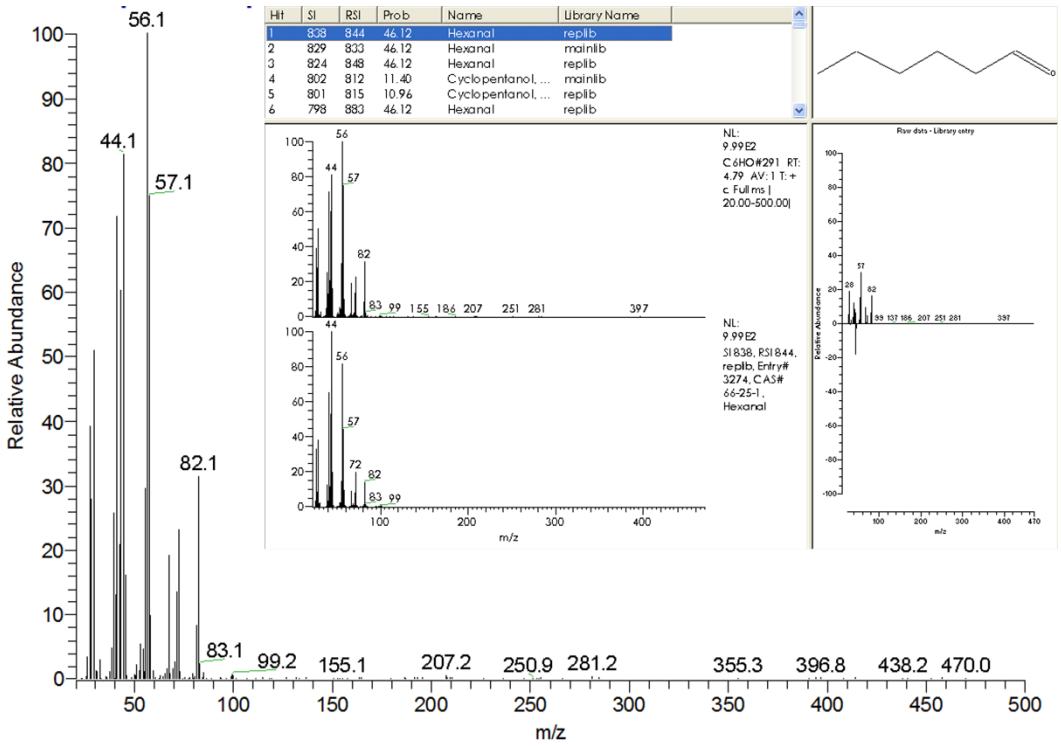

Figure S9. MS spectrum of Caproaldehyde.

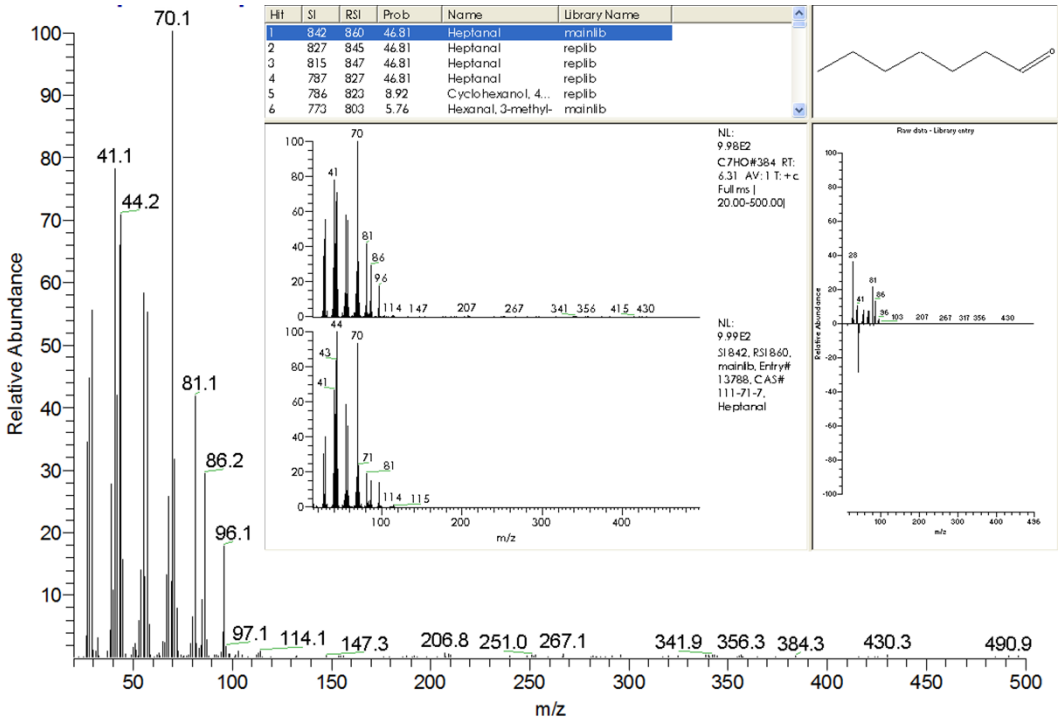

Figure S10. MS spectrum of Heptaldehyde.

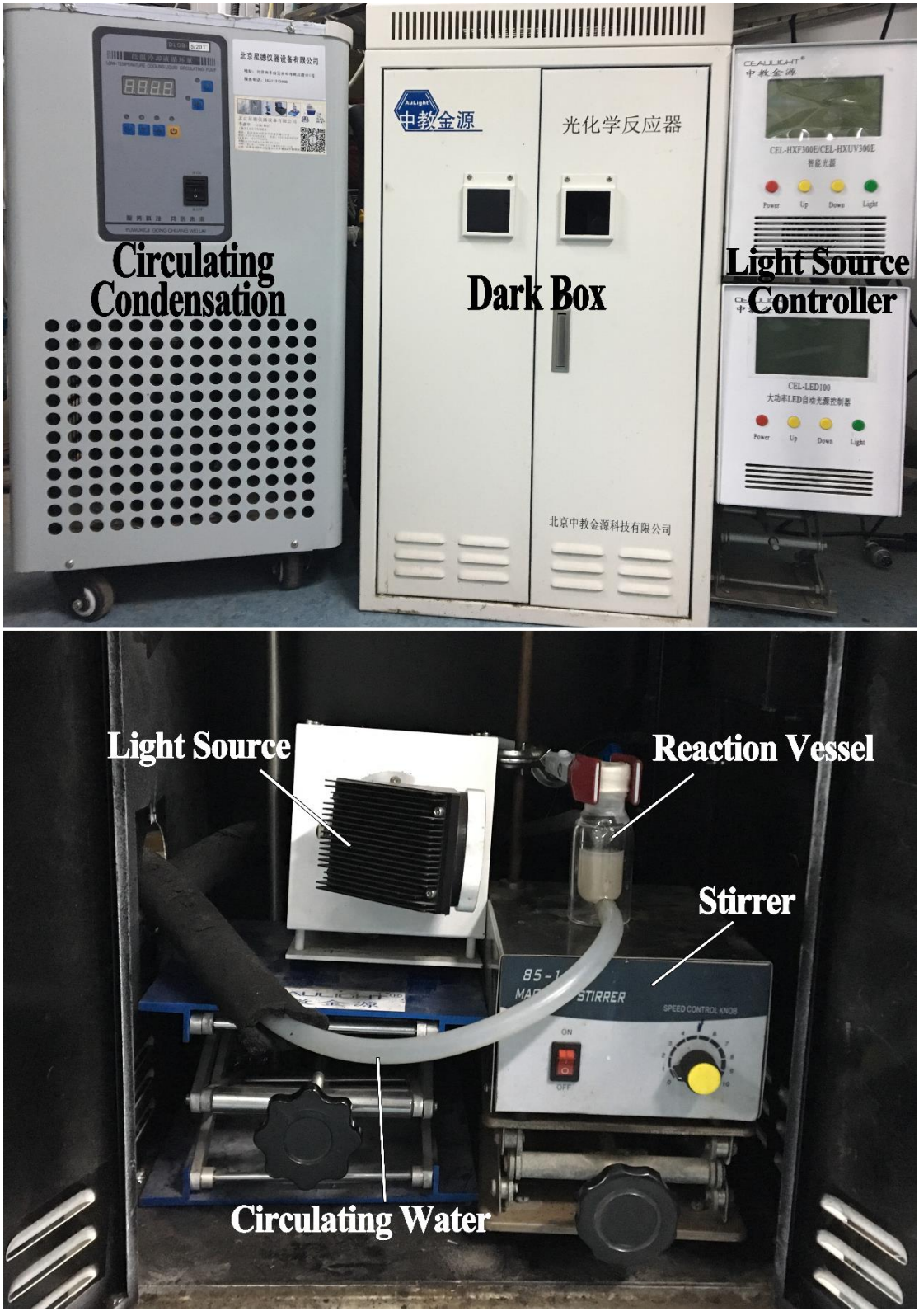

Figure S11. Photoreaction equipment of photocatalytic experiment process.

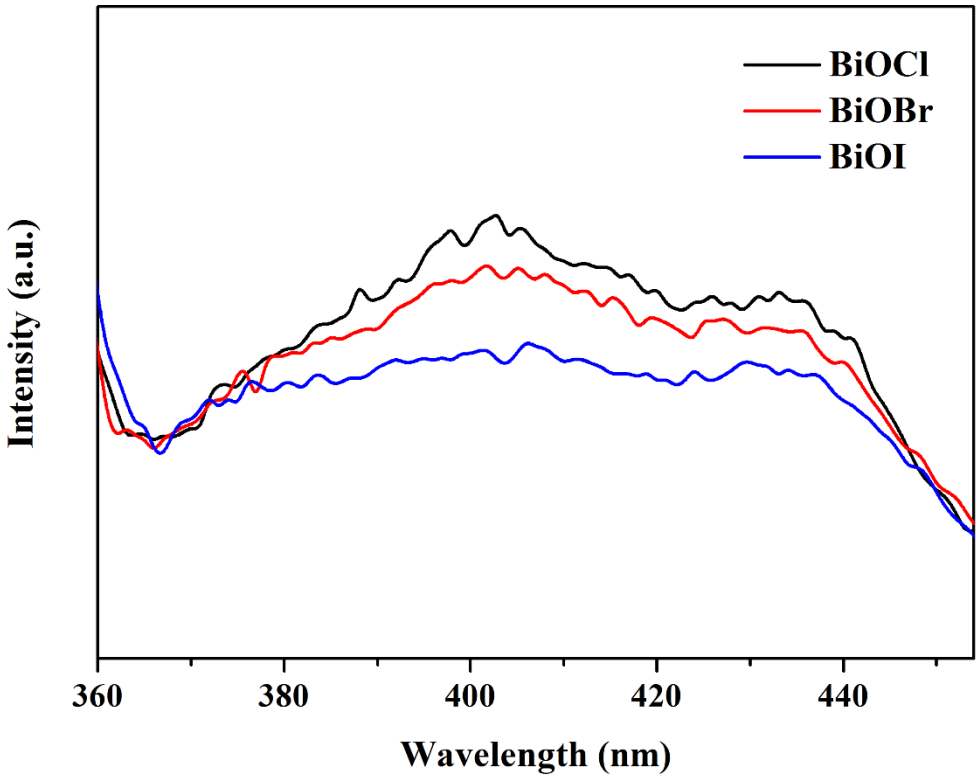

Figure S12. Fluorescence detection of the generated H_2O_2 after oxidation reaction over BiOCl, BiOBr, and BiOI.